



Morphology tunable organogels based on dihydrazide derivatives

Binglian Bai ^{a,b,*}, Jue Wei ^b, Jian Zhao ^b, Haitao Wang ^a, Min Li ^{a,**}

^a Key Laboratory for Automobile Materials (JLU), Ministry of Education, Institute of Materials Science and Engineering, Jilin University, Changchun 130012, PR China

^b College of Physics, Jilin University, Changchun 130012, PR China

ARTICLE INFO

Article history:

Received 21 February 2012

Received in revised form 17 May 2012

Accepted 2 July 2012

Available online 11 July 2012

Keywords:

Organogels

Dihydrazide derivatives

Hydrogen bonding

Supramolecular chains

ABSTRACT

We report on the organogels of a new series of compounds containing a dihydrazide unit in the rigid core and three long alkoxy chains. SEM images revealed that the morphologies of the xerogels strongly depend on the polarity of the gelling solvent. Textured spheroid-like morphologies were observed in the xerogels from low polar aromatic solvents such as benzene, whereas fibrous morphologies from ethanol. Further detailed analysis of their aggregation modes was conducted by FT-IR and X-ray diffraction measurement. The cooperation of hydrogen bonds, hydrophobic interactions and the van der Waals interactions should be the key point of the self-assembly.

© 2012 Elsevier B.V. All rights reserved.

1. Introduction

The organogels are a class of nanostructured materials composed of a self-assembled superstructure of the low molecular weight organogelators through specific noncovalent intermolecular interactions including hydrogen bonds, hydrophobic interactions, π - π interactions, or Van der Waals forces and a large volume of organic liquid immobilized therein [1]. In order for the formation of organogels, it is important to control the noncovalent intermolecular interactions in such a way to avoid transformation to isotropic solution or crystalline state.

Among the noncovalent interactions, hydrogen bonding was the most commonly used to direct the self-assembly process. Well-known organogelators such as derivatives of carbohydrates [2,3], amino acids [4,5], and urea [6,7], have been revealed to self-assemble through hydrogen bonding interactions into long fibrous structures, which in turn form an entangled network and thus immobile solvents therein.

The morphologies of the gels depend on many factors such as molecular structures of gelators, the ratio of the gelators in two-component systems, or external stimulus (temperature, ultrasound etc.) [8]. However, the report on solvents impacting on the morphologies of the gels is relatively rare. Recently, John et al. [9] found that the morphology of gels was different depending on the solvents, and both fibrous networks and sheets were observed in different solvents. Huang et al. [10] reported the morphology of an azobenzene derivative exhibited regular flakes

connected by thin ribbons in 1-butanol, while homogeneous cabbage like spherical structures in xylene.

Recently, we reported the synthesis and mesophase from non-symmetrical tapered hydrazide derivatives, *N*-(3,4,5-trialkoxybenzoyl)-*N'*-(4'-aminobenzoyl) hydrazine (Dn) [11] as shown in Scheme 1, which formed stable columnar mesophase driven by N-H...O=C intermolecular double H-bonding. In this work, we report gelation behaviors of Dn ($n=6$ and 16), and the compound *N*-(3,4,5-trihexadecyloxybenzoyl)-*N'*-(4'-aminobenzoyl) hydrazine (D16) showed strong gelation ability in some organic solvents. Notably, the morphologies of the organogels are tunable by the polarity of the gelling solvent.

2. Experimental

2.1. Gelation experiments

The weighted powder compound and solvent were sealed in a little glass tube, and were then gently heated to make the gelator completely dissolved. The resulting solution was cooled in air at about 4 °C (or 20 °C) for several minutes, and then the gelation was checked visually. When upon inversion of the test tube no fluid ran down the walls of the tube, we judge its "gelation". The xerogels were obtained through slowly evaporating the solvents from organogels, which were kept in air at about 4 °C.

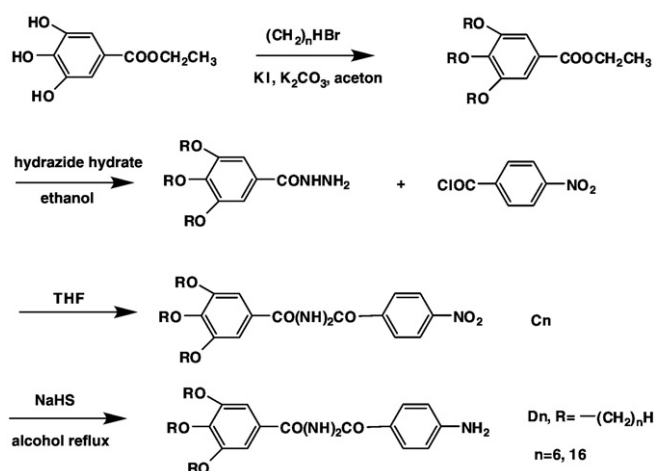
2.2. Characterization

FT-IR spectra were recorded with a Perkin-Elmer spectrometer (Spectrum One B). The sample was pressed tablet with KBr. X-ray diffraction was carried out with a Bruker Avance D8 X-ray diffractometer.

* Correspondence to: B. Bai, Key Laboratory for Automobile Materials (JLU), Ministry of Education, Institute of Materials Science and Engineering, Jilin University, Changchun 130012, PR China. Tel.: +86 431 85168254.

** Corresponding author. Tel.: +86 431 85168254.

E-mail addresses: baibinglian@jlu.edu.cn (B. Bai), minli@mail.jlu.edu.cn (M. Li).



Scheme 1. The synthesis of compounds Dn.

SEM observations were taken with SSX-550 and JSM-6700F apparatus. Samples for SEM study were xerogels. Transmission electron microscopy (TEM) morphology was obtained with JEM 2010 apparatus. Samples for TEM study were prepared by dropping a small amount of solution onto a 400-mesh copper grid followed by evaporating the solvent at ambient temperature. Thermal gravimetry (TG) curves were measured on a TA SDTQ 600 instrument.

3. Results and discussion

3.1. Thermal behavior of the organogels

Interestingly, only D16 with long alkyl chains showed strong gelation ability in organic solvents such as ethanol, benzene, 1,2-dichloroethane et al. (Table 1), while D6 with short alkyl chains cannot gel any of the above solvents. D16 exhibits strong gelation ability in ethanol and the gelation occurs even at 0.14 wt%. Whereas the minimum gel concentration of D16 in benzene appears at 1.3 wt% suggesting its weak gelation ability. Fig. 1 shows the gel–sol transition temperature (T_{gel}) of D16 gel in ethanol as a function of concentration. The T_{gel} increases from 52 °C to 67 °C as the concentration of D16 increases from 0.65 wt.% to 2.98 wt.%.

3.2. Morphological properties of organogelator D16

The morphologies of the corresponding xerogels were investigated by scanning electron microscopy (SEM). Fig. 2 shows the SEM images of the organogels in different solvents. Interestingly, the morphologies of the xerogels are different in different solvents. For example, the D16 xerogels from benzene showed the surface-patterned, clumped, and textured spheroids (Fig. 2a, b, c), with the diameters of 5–10 μ m. The diameters of the textured spheroids remain almost unchanged,

Table 1

Gelation properties of D16 (G: gel, S: solution, PG: partial gel, CGC: values mean critical gelation concentration necessary for gelation).

Solvents	State	CGC	
		4 °C	20 °C
Tetrahydrofuran	S		
Ethanol	G	0.14%	0.6%
Methanol	PG		
Chloroform	S		
1,2-Dichloroethane	G	0.87%	1.1%
Benzene	G	1.3%	3.4%
Toluene	G	2.5%	2.7%
Dimethylbenzene	G	3.79%	S

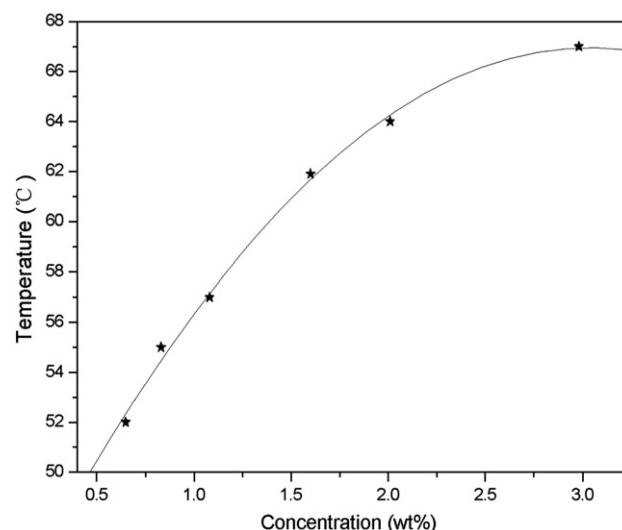
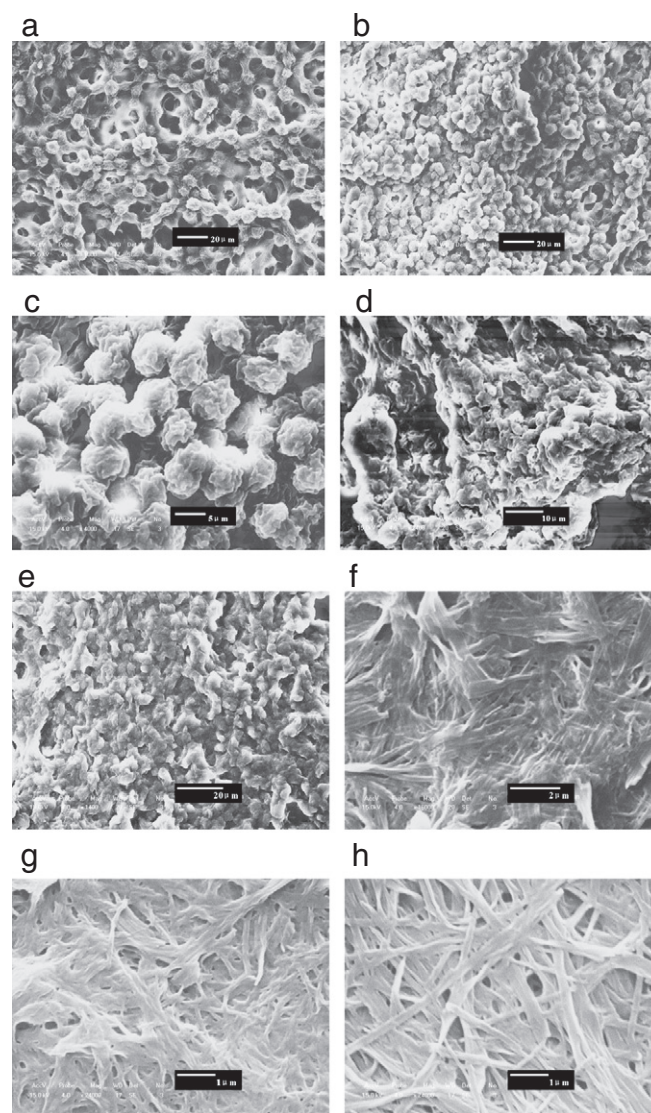
Fig. 1. Concentration-dependent T_{gel} of D16 gels in ethanol.

Fig. 2. SEM images of D16 xerogels from (a) benzene (1.30 wt%), (b) benzene (3.39 wt%), (c) benzene (3.39 wt%), (d) toluene (11.5 wt%), (e) dimethylbenzene (3.79 wt%), (f) methanol (0.83 wt%), (g) ethanol (0.56 wt%), and (h) ethanol (1.11 wt%).

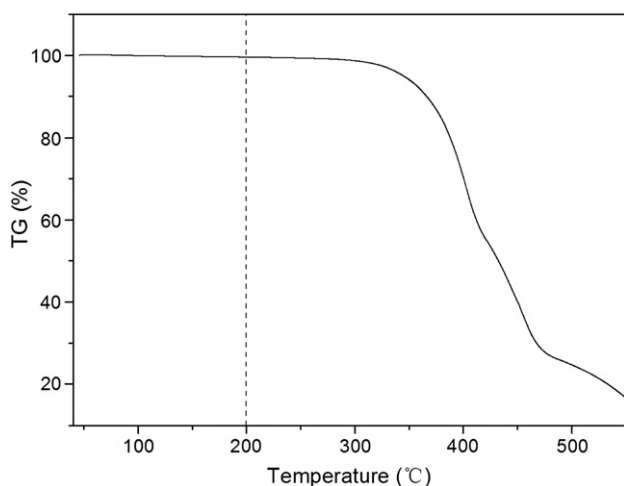


Fig. 3. TGA curve of D16 xerogel from ethanol (2.22 wt.%).

but its density increases obviously with the increase of the concentration from 1.30% to 3.39%. In contrast, the xerogels of D16 in ethanol exhibit networks composed of straight bundles of fibers (Fig. 2g, h) and the fibrous diameters increase obviously with the increase of the concentration from 0.56% to 1.11%. In the thermal gravimetric analysis (TGA) on xerogel of D16, no losses of thermogram weight were detected upon heating to its isotropic point (138 °C), indicating that there is no ethanol in the xerogel (Fig. 3).

To clarify and confirm the original structure of the gel in benzene, TEM morphology of D16 in benzene solution was investigated (Fig. 4). Thin fibers with tens of nanometers in diameter were observed, suggesting that molecules self-assemble nanofibers in benzene solution.

The formation of elongated fiber-like aggregates indicates that the self-assembly of D16 is driven by strong directional intermolecular interactions. To ascertain whether hydrogen bonding plays a role in the gelation process, infrared spectrum of the organogels was examined. Fig. 5 shows IR spectra of the xerogels from benzene and ethanol in the range of 3800–2750 and 1800–1500 cm^{-1} . The observation of hydrogen bonded N–H stretching bands (3206 cm^{-1} (benzene gel) and 3223 cm^{-1} (ethanol gel)), intense absorption of bonded C=O stretching vibrations (1627 cm^{-1} and 1561 cm^{-1}) clearly indicates that the N–Hs of the central hydrazide group are associated with

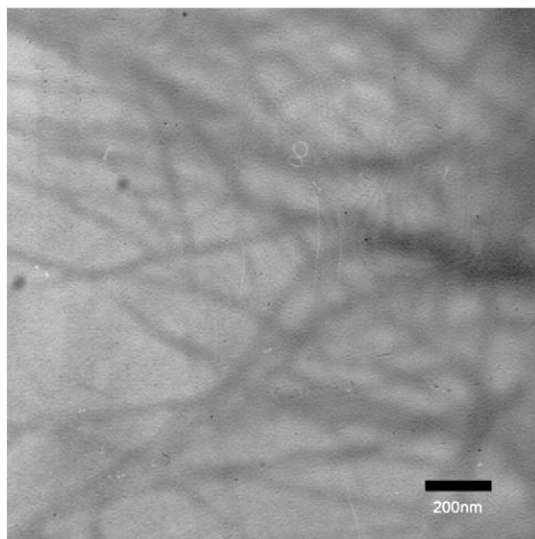


Fig. 4. TEM image of D16 in benzene solution (0.18 wt.%).

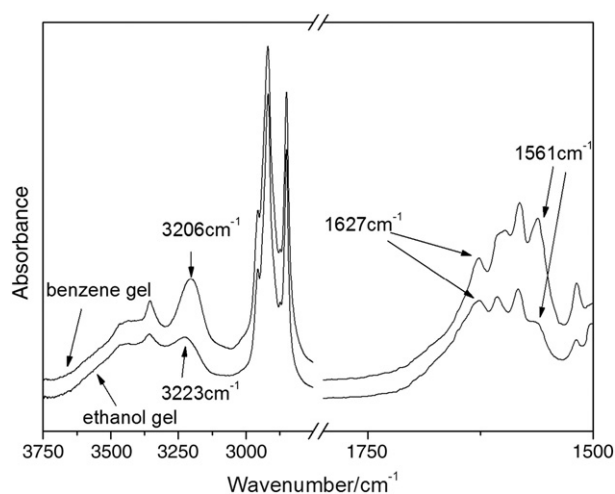


Fig. 5. FT-IR spectra of the xerogels of D16 from benzene (3.39 wt.%) and ethanol (1.11 wt.%).

the C=O groups via N–H...O=C intermolecular hydrogen bonding in the gelation process and the intensity of the intermolecular hydrogen bonding in the xerogels from benzene is stronger than that of ethanol [12,13], such hydrogen bonding interaction was considered to be the main driving forces for the formation of the fibers. In addition, the absorption bands of the antisymmetric (ν_{as}) and symmetric (ν_{s}) CH_2 stretching vibrational modes are observed at 2918 cm^{-1} (ν_{as} CH) and 2850 cm^{-1} (ν_{s} CH) in the gel, respectively, indicating that the alkyl chains are ordered in part and there is a strong organization of the alkyl groups via van der Waals interaction [14]. The intermolecular hydrogen bonding of the central hydrazide group as well as the amino head groups can also be confirmed by concentration-dependent ^1H NMR measurements [11].

Fig. 6 shows the X-ray diffraction patterns of D16 xerogel from ethanol and benzene. The XRD pattern of D16 xerogel from benzene exhibited one strong peak ($d = 59.1 \text{ \AA}$) and two weak peaks at 29.4 (200) and 14.7 (400) \AA in the low-angle range, suggesting a layer structure. In the high-angle regions, two diffuse broad peaks with a maximum at about 4.0 and 4.5 \AA , suggesting the coexistence ordered and disordered feature. The peak at 4.5 \AA is characteristic of the aliphatic chains, while that at 4.0 \AA might be attributed to the repeat distance of hydrazide units in stacking [12d]. The layer spacing from

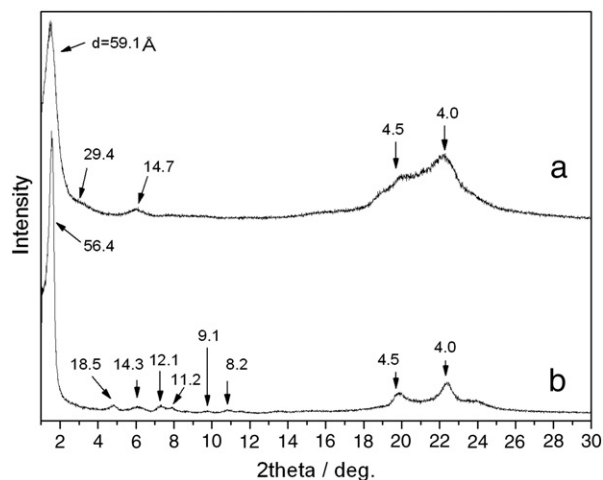
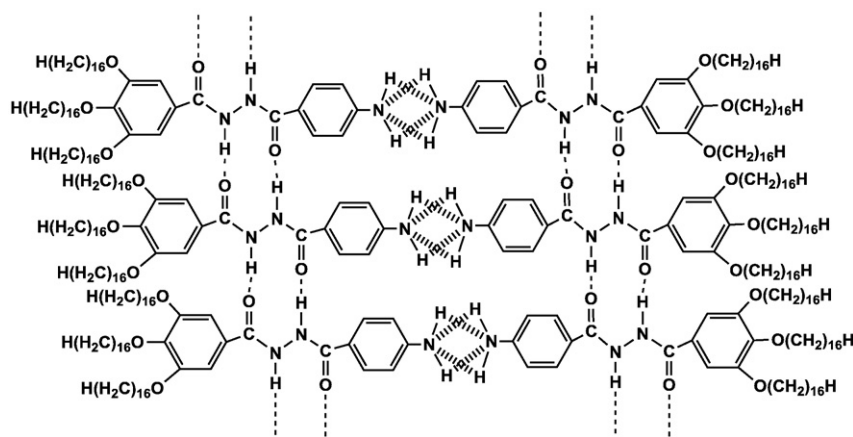


Fig. 6. X-ray diffraction patterns of the benzene xerogels (3.39 wt.%) (a), and the ethanol xerogels (1.11 wt.%) (b).



Scheme 2. Schematic representation of D16 self-assembling to supramolecules (the dashed line illustrates the hydrogen bonding).

XRD is much larger than the calculated full extended molecular length (about 33.3 Å) and smaller than twice the calculated full extended molecular length. And considering the results of the ^1H NMR diluting experiment [11] and FTIR spectroscopy, the molecules should self-assemble into supramolecular chains through intermolecular hydrogen bonding (Scheme 2) and they have a little tilt angle in layers. Whereas many sharp diffraction peaks in the low-angle range were observed for D16 xerogels in ethanol indicating the structure in ethanol gel was more ordered than that of benzene gel.

Combining the above results, the process of gel formation can be explained on the assumption that the molecular self-assembled to form supramolecular chains mainly through intermolecular hydrogen bonding interactions, namely elemental fibrils, which hierarchically assembled to fibrous bundles, and farther to textured spheroids (in benzene gel) or more thicker fibrous bundles (in ethanol gel). Why the morphologies of xerogels have much difference? These morphological features are determined by the extent of the solvent–gelator interactions. In benzene gel, because of the hydrophobic interactions, the nonpolar benzene solvent is apt to penetrate and interact with the peripheral nonpolar group, namely the phenyl rings with trialkoxy groups as well as alkyl chains, the solvent–gelator interaction makes the fibrils interconnect each other and conglutinate to form sheet, thereby loss of fibrous unidirectional orientation, meanwhile, the strong hydrogen bonding interactions of gelator–gelator as well as the penetration into layer of benzene solvent make the sheet “curl” and divert from the plane, so the isotropic aggregation occurs, resulting in complete loss of fibrous structure and less stable gels. While the polar ethanol solvent is apt to interact with the polar group namely dihydrazide groups, and takes part in the hydrogen bonding, meanwhile impairs the intermolecular hydrogen bonding interactions of gelator–gelator to some extent, thus the macroscopic morphology maintains fibrous characters, resulting in high gelation ability and stable gels.

4. Conclusion

We have demonstrated the unique self-assembling ability of a novel gelator D16, which showed strong gelation abilities in some organic solvents. The morphologies of the xerogels prepared from this gelator strongly depend on the polarity of the gelling solvent. Results from FTIR spectroscopy revealed that intermolecular H-bonds are the main driving force for the formation of supramolecular chains. The cooperation of hydrogen bonds, microsegregation effect, hydrophobic interactions and the van der Waals interactions is the key point of the self-assembly. Competitive or cooperative interactions of gelator–gelator and solvent–gelator could control the morphology of one-component self-assembled organogel materials, which provide

new opportunities to one-component low weight molecular (LWM) materials.

Acknowledgment

The authors are grateful to the National Science Foundation Committee of China (project Nos. 21072076, 51103057, 51073071), the Special Foundation for PhD Program in Universities of China Ministry of Education (Project No. 20090061120021), and Project 985-Automotive Engineering of Jilin University for their financial support to this work.

References

- (a) M. George, R.G. Weiss, *Chemistry of Materials* 15 (2003) 2879–2888;
- (b) M. George, R.G. Weiss, *Langmuir* 18 (2002) 7124–7135;
- (c) P. Zhang, H. Wang, H. Liu, M. Li, *Langmuir* 26 (2010) 10183–10190;
- (d) L. Su, C. Bao, R. Lu, Y. Chen, T. Xu, D. Song, C. Tan, T. Shi, Y. Zhao, *Organic and Biomolecular Chemistry* 4 (2006) 2591–2594;
- (e) X. Zhang, R. Lu, J. Jia, X. Liu, P. Xue, D. Xu, H. Zhou, *Chemical Communications* 46 (2010) 8419–8421;
- (f) T.H. Kim, D.G. Kim, M. Lee, T.S. Lee, *Tetrahedron* 66 (2010) 1667–1672.
- (a) C.Y. Bao, R. Lu, M. Jin, P.C. Xue, C.H. Tan, Y.Y. Zhao, G.F. Liu, *Carbohydrate Research* 339 (2004) 1311–1316;
- (b) C.Y. Bao, R. Lu, M. Jin, P.C. Xue, C.H. Tan, Y.Y. Zhao, G.F. Liu, *Journal of Nanoscience and Nanotechnology* 4 (2004) 1045–1051.
- (a) G. John, J.H. Jung, H. Minamikawa, K. Yoshida, T. Shimizu, *Chemistry A European Journal* 8 (2002) 5494–5500;
- (b) A. Friggeri, O. Gronwald, K.J.C. van Bommel, S. Shinkai, D.N. Reinhoudt, *Journal of the American Chemical Society* 124 (2002) 10754–10758.
- M. Suzuki, M. Yumoto, M. Kimura, H. Shirai, K. Hanabusa, *Chemistry A European Journal* 9 (2003) 348–354.
- M. Suzuki, T. Nigawara, M. Yumoto, M. Kimura, H. Shirai, K. Hanabusa, *Tetrahedron Letters* 44 (2003) 6841–6843.
- K. Yabuuchi, E. Marfo-Owusu, T. Kato, *Organic and Biomolecular Chemistry* 1 (2003) 3464–3469.
- (a) J.V. Esch, F. Schoonbeek, M.D. Looks, H. Kooijman, A.L. Spek, R.M. Kellogg, B.L. Feringa, *Chemistry A European Journal* 5 (1999) 937–950;
- (b) L.A. Estroff, A.D. Hamilton, *Angewandte Chemie International Edition* 39 (2000) 3447–3450;
- (c) K. Hanabusa, K. Shimura, K. Hirose, M. Kimura, H. Shirai, *Chemistry Letters* 10 (1996) 885–886.
- (a) A.R. Hirst, D.K. Smith, M.C. Feiters, H.P.M. Geurts, A.C. Wright, *Journal of the American Chemical Society* 125 (2003) 9010–9011;
- (b) A.R. Hirst, D.K. Smith, J.P. Harrington, *Chemistry A European Journal* 11 (2005) 6552–6559;
- (c) A.R. Hirst, D.K. Smith, *Chemistry A European Journal* 11 (2005) 5496–5508;
- (d) Y. Zhou, M. Xu, T. Yi, S. Xiao, Z. Zhou, F. Li, C. Huang, *Langmuir* 23 (2007) 202–208;
- (f) M.A. Rogers, A.J. Wright, A.G. Marangoni, *Current Opinion in Colloid and Interface Science* 14 (2009) 33–42;
- (g) J. Wu, T. Yi, T. Shu, M. Yu, Z. Zhou, M. Xu, Y. Zhou, H. Zhang, J. Han, F. Li, C. Huang, *Angewandte Chemie International Edition* 47 (2008) 1063–1067;
- (h) X. Yu, Q. Liu, J. Wu, M. Zhang, X. Cao, S. Zhang, Q. Wang, L. Chen, T. Yi, *Chemistry A European Journal* 16 (2010) 9099–9106.
- G. John, J.H. Jung, M. Masuda, T. Shimizu, *Langmuir* 20 (2004) 2060–2065.
- Y. Zhou, T. Yi, T. Li, Z. Zhou, F. Li, W. Huang, C. Huang, *Chemistry of Materials* 18 (2006) 2974–2981.

- [11] B. Bai, C. Zhao, H. Wang, X. Ran, D. Wang, M. Li, *Materials Chemistry and Physics* 133 (2012) 232–238.
- [12] (a) B. Bai, H. Wang, H. Xin, F. Zhang, B. Long, X. Zhang, S. Qu, M. Li, *New Journal of Chemistry* 31 (2007) 401–408;
(b) S. Qu, F. Li, H. Wang, B. Bai, C. Xu, L. Zhao, B. Long, M. Li, *Chemistry of Materials* 19 (2007) 4839–4846;
(c) P. Zhang, S. Qu, B. Bai, H. Wang, X. Ran, C. Zhao, M. Li, *Liquid Crystals* 36 (2009) 817–824;
(d) P. Zhang, H. Wang, H. Liu, M. Li, *Langmuir* 26 (2010) 10183–10190;
(e) H. Wang, B. Bai, D. Pang, Z. Zou, L. Xuan, F. Li, P. Zhang, L. Liu, B. Long, M. Li, *Liquid Crystals* 35 (2008) 333–338.
- [13] (a) H. Gunzler, H. Gremlich, *IR Spectroscopy*, Wiley-VCH, 2002.;
(b) L.J. Bellamy, 3rd ed., *The Infra-red Spectra of Complex Molecules*, vol. 1, Chapman & Hall Ltd., 1975.;
(c) K. Kurihara, K. Ohto, Y. Honda, T. Kunitake, *Journal of the American Chemical Society* 113 (1991) 5077–5079.
- [14] M. Suzuki, Y. Nakajima, M. Yumoto, M. Kimura, H. Shirai, K. Hanabusa, *Langmuir* 19 (2003) 8622–8624.